Interaction Potentials, Spectroscopy and Transport Properties of $C^+(^2P_J)$ and $C^+(^4P_J)$ with Helium

Abstract

We calculate accurate interatomic potentials for the interaction of a singly-charged carbon cation with a helium atom. We employ the RCCSD(T) method, and basis sets of quadruple-ζ and quintuple-ζ quality; each point is counterpoise corrected and extrapolated to the basis set limit. We consider the two lowest $C^+(^2P)$ and $C^+(^4P)$ electronic states of the carbon cation, and calculate the interatomic potentials for the terms that arise from these: $^2\Pi$ and $^2\Sigma^+$, and $^4\Pi$ and $^4\Sigma^-$, respectively. We additionally calculate the interatomic potentials for the respective spin-orbit levels, and examine the effect on the spectroscopic parameters. Finally, we employ each set of potentials to calculate transport coefficients, and compare these to available data. Critical comments are made in the cases where there are discrepancies between the calculated values and measured data.

Authorship:

William D. Tuttle,[a] Rebecca L. Thorington,[a] Larry A. Viehland,[b *] and Timothy G. Wright [a **]

[a] School of Chemistry, University Park, University of Nottingham, Nottingham NG7 2RD, United Kingdom.

[b] Science Department, Chatham University, Pittsburgh, Pennsylvania 15232, USA

* **Email**: Viehland@Chatham.edu

** **Email**: Tim.Wright@nottingham.ac.uk

I. Introduction

Carbon ions, C^+, appear in wide-ranging situations, including flames and plasmas,[1] chemical vapour deposition (CVD)[2] and for use in radiotherapy.[3] They are also possibly present in small amounts in the ionospheres of the Earth[4] and those of other planets;[5] additionally, they are thought to play a key role in the chemistry of the interstellar medium.[6] Chemistry mostly starts with interactions between species, and the interactions of atomic cations with rare gas atoms are generally agreed to be amongst the simplest interactions that can be probed, especially when the rare gas is the very non-polarizable helium atom. Indeed, the C^+-He complex has been proposed as a possible species in the interstellar medium by Harrison *et al.*[7] and interactions between C^+ and He could be a cooling mechanism for C^+ ions in the interstellar medium and dense interstellar clouds.[8]

Interatomic potentials are also important in the calculation of a range of quantities including collision cross sections – important in the calculation of ion transport data – and atomic collisional energy transfer. In turn, these underpin knowledge of: transport time and loss mechanisms to walls in flow-tube experiments, transport of ions in plasmas, CVD, and cooling of interstellar clouds.

Here we investigate the interatomic potentials that arise from the lowest two atomic asymptotes of the open-shell C^+-He complex, $C^+(^2P_J)$ + He($^1S_0$) and $C^+(^4P_J)$ + He($^1S_0$). From these we shall obtain accurate spectroscopic constants and transport coefficients to determine whether the spin-orbit (SO) interaction affects these significantly. The present work also serves as a precursor to the study of higher atomic number Group 14 atomic cation-rare gas species, where the inclusion of the SO interaction is certainly expected to be important in an accurate description of the interaction potentials.

When He interacts with C^+, the degenerate atomic states are split. In the absence of the spin-orbit interaction, the ^2P ground electronic term of C^+ gives rise to lower $^2\Pi$ and higher $^2\Sigma^+$ diatomic terms, and the first excited ^4P atomic state of carbon leads to lower $^4\Sigma^-$ and higher $^4\Pi$ diatomic terms. These are the states that have been investigated by previous theoretical investigations, but it is the spin-orbit split levels that are probed experimentally.

Upon the inclusion of the spin-orbit (SO) interaction, $C^+(^2P)$ splits into a lower $^2P_{1/2}$ and a higher $^2P_{3/2}$ level, with a separation of 63.42 cm^{-1} (Ref. 9). The SO interaction causes the $^2\Pi$ diatomic term to split into $^2\Pi_{1/2}$ and $^2\Pi_{3/2}$ levels, and the $^2\Sigma^+$ term to become $^2\Sigma_{1/2}{}^+$; the lowest $^2\Pi_{1/2}$ level correlates to the $C^+(^2P_{1/2})$ + He($^1S_0$) asymptote, while the middle $^2\Pi_{3/2}$ and upper $^2\Sigma_{1/2}{}^+$ levels both correlate to $C^+(^2P_{3/2})$ + He($^1S_0$).

For the excited $C^+(^4P)$ ion, there are three SO levels; the lowest is $^4P_{1/2}$, the middle $^4P_{3/2}$ is higher by 22 cm^{-1}, and the upper $^4P_{5/2}$ lies another 50.3 cm^{-1} higher (Ref. 9). The spin-orbit interaction leads to the $^4\Pi$ diatomic state splitting into $^4\Pi_{-1/2}$, $^4\Pi_{1/2}$, $^4\Pi_{3/2}$ and $^4\Pi_{5/2}$ levels, where it should be noted that here $\Omega = \Lambda+\Sigma$ rather than $\Omega = |\Lambda+\Sigma|$ is employed to allow for the $\Omega = -^1/_2$ level to be differentiated from the $\Omega = {}^1/_2$ one. This follows the convention used by Herzberg in his classic text.[10] The $^4\Sigma^-$ state gives rise to two levels, corresponding to $\Omega = ½$ and $\Omega = {}^3/_2$.

Since Ω levels of the same value can mix, an interaction between the $^2\Pi_{1/2}$ and $^2\Sigma_{1/2}{}^+$ levels is expected. The mixing of these is expected to be small, and so we will refer to the resulting $\Omega = {}^1/_2$ levels with the original $^2\Pi_{1/2}$ and $^2\Sigma_{1/2}{}^+$ labels, rather than relabelling the linear combinations which result; similar comments refer to the quartet states. Other smaller mixings can also occur with higher energy states, and indeed between the doublet and quartet states with the same value of Ω; however, since the separation between such manifolds of state exceed 30,000 cm^{-1}, these are neglected here. To simplify the presentation, we shall use the word "state" to refer to atomic and molecular terms or levels, with the term symbol or context making it clear which is being referred to.

There has been significant work on the C^+-He complex over the past 40 years, including calculating equilibrium internuclear separations, spectroscopic constants and binding energies of the systems, as well as measuring transport data for the carbon cation in rare gases. The first such studies appear to be the almost contemporaneous papers by Toshima[8] and Harrison *et al.*[7] The former constructed potentials from attractive and repulsive terms, yielding curves for $^2\Pi_{3/2}$, $^2\Pi_{1/2}$ and $^2\Sigma_{1/2}{}^+$; however, no spectroscopic parameters were reported. Harrison *et al.*[7] used Hartree-Fock theory to calculate a potential energy curve for the $^2\Pi$ state; it was noted therein that this was only presumed to be the ground state, and that the calculations for the $^2\Sigma^+$ state did not converge. Both of these studies were prompted by interest in C^+ in the interstellar medium, with Harrison *et al.* suggesting it may be possible to detect the C^+-He complex in interstellar space, while Toshima concluded that C^+/He collisions could be important in cooling within dense interstellar clouds.

Cooper and Wilson[11] also studied C^+-He by the Hartree-Fock method in 1981, where they were able to obtain curves for both the $^2\Pi$ and $^2\Sigma^+$ states, confirming that indeed the $^2\Pi$ state was lower in energy. In 1986, Young and Coggiola[12] made the first mass spectrometric observation of a stable ion involving helium, which they postulated to be either $[CHe]^+$ or $[C_2He_2]^{2+}$. A number of quantum chemical calculations then followed, using various split-valence Pople-style basis sets. The first report using correlated methods was by Koch and Frenking[13] in 1986 using the MP2 method, these were followed by a short communication using the MP4 method by Wong *et al.*[14] Wider-ranging MP2

studies across the first row mono- and dications were also reported a few years later by Frenking *et al.*,[15] with single-point MP4 calculations being employed for more reliable binding energies.

Most of these papers only reported equilibrium interatomic separations, rather than potential energy curves as such; even the reported curves[7,8] were quite limited. Similarly limited curves at the MP4(SDQ) level were reported by Grice *et al.*[16], who looked at potentials arising from each of the ^2P and ^4P states of C^+ interacting with He. Jemmis *et al.*[17] calculated the internuclear separation at both the MP2 and QCISD(T) levels, while Hughes and von Nagy-Felsobuki[18] calculated the same at the CCSD(T)/cc-pVQZ level, and also reported harmonic vibrational frequencies. Finally Matoba *et al.*[19] calculated interaction potentials for the $^2\Pi$, $^2\Sigma^+$, $^4\Sigma^-$ and $^4\Pi$ states using the MRCI/d-aug-cc-pVQZ approach with transport data and spectroscopic constants also being reported.

Early measurements, in 1979, of C^+ ion mobilities at ~300 K in He were made by Thomas *et al.*[20] (who also measured $ND_{L,}$ the longitudinal diffusion coefficient multiplied by the gas number density) and Dotan *et al.*,[21] both concentrating on the $C^+(^2P)$ ground state. (A smoothed version of the Dotan *et al.* data has been presented in ref. 22.) Data given in a 1981 thesis by Peska[23] are also available for $C^+(^2P)$ ion mobilities in He. A later study in 1986 by Twiddy *et al.*[24] reported measurements on both $C^+(^2P)$ and the metastable $C^+(^4P)$ ions; this is one of the few mobility studies to observe excited state ions. The potentials and calculated ion mobilities of Grice *et al.*[16] supported the observations by Twiddy *et al.*[24] of $C^+(^4P)$ in their flow-drift tube experiment. More recently, Matoba *et al.*[19] studied the mobility of $C^+(^2P)$ and $C^+(^4P)$ at 77 and 4.3 K. They also used their calculated MRCI/d-aug-cc-pVQZ interaction potentials to calculate ion mobilities and compared these to their experimental data.

We also note that Rincon *et al.*[25] have studied the translational energy spectroscopy of ion beams containing $C^+(^2P)$ and $C^+(^4P)$. Collisions between these beams and neutral molecules as well as He were undertaken, which allowed the proportion of the different states to be determined. Further, it was found that spin-changing collisions only occurred with an open-shell collision partner, while closed-shell partners resulted in spin being conserved.

II. Computational Methodology

A. Quantum Chemistry

Interaction potentials with and without the spin-orbit interaction have been computed for all diatomic states arising from the lowest two atomic asymptotes of C^+-He in the following manner. Energies at more than 100 internuclear separations from 0.8 to 50 Å were evaluated at the RCCSD(T) level of

theory as implemented in MOLPRO;[26,27] all electrons were correlated. Standard aug-cc-pwCVXZ[28] and aug-cc-pVXZ (X=Q, 5)[29] basis sets were used for carbon and helium respectively, and the interaction energies at each separation were counterpoise-corrected to account for basis set superposition error. Finally, the interaction potentials were point-by-point extrapolated to the basis set limit utilising the two-point (cubic) formula of Halkier *et al.*[30,31] at each separation; for simplicity, we denote the final potentials as RCCSD(T)/aV∞Z. These interaction energies were then used as the unperturbed eigenvalues of the Breit-Pauli spin-orbit matrix as implemented in MOLPRO to allow calculation of RCCSD(T) interaction energies inclusive of spin-orbit splitting at each separation.[32] From each interaction energy curve, the rovibrational energy levels were obtained using the LEVEL program.[33] The lowest two relevant levels were used in each case to obtain the spectroscopic constants from standard formulae.

We note that the potentials were calculated with a high precision in MOLPRO, with the integrals converging to within 10^{-12} E_h, energy converging to 10^{-12} E_h, orbitals in the SCF program to 10^{-8} and the CCSD coefficients to 10^{-7}. Our T_1 diagnostic values are ~0.02 for the ^2P state and ~0.04 for the ^4P state; these values are acceptable, but we also note that good agreement is seen with previously-reported MRCI values with similar basis sets, confirming that multireference behaviour is not unduly affecting our potentials.

B. Transport Coefficients

We calculated the transport cross sections for C^+ in He from the *ab initio* interaction potential energy curves as functions of the ion-neutral collision energy using the classical-mechanical program PC[34] that is an improved version of the earlier program QVALUES.[35,36] The cross sections converged within 0.05%.

The cross sections as a function of collision energy were used in the program GC[35,37,38] to determine the standard mobility, K_0, and the other gaseous ion transport coefficients as functions of E/n_0 (the ratio of the electric field to the gas number density) at gas temperatures, T, of 4.35, 77, 100, 200, 300, 400 and 500 K. We also used program VARY[39] to determine the zero-field value of K_0 as a function of T from 0.001 to 10000 K. Calculations were performed for both $^{12}C^+$ and $^{13}C^+$, while He was assumed to be the naturally-occurring mixture of isotopes. The calculated mobilities are generally precise within the precision of the cross sections at E/n_0 values below 20 Td (1 Td = 10^{-21} V m^2). The results are progressively less precise as E/n_0 increases to 1000 Td, but these details, as well as the mobilities and other transport properties, can be obtained from the tables placed in the database that is maintained from the University of Toulouse.[40] Various weightings of the cross-sections were employed for each system, and these will be stated at the appropriate points below.

Additionally, it should be noted that each spin-orbit interaction potential was shifted such that the interaction energies computed at the longest internuclear separation, 100 Å, were equal to the $1/R^4$ ion-induced dipole interaction energy at this separation. This was done so that the asymptotes smoothly approached zero energy for the transport calculations; this shift has a negligible effect on the spectroscopic constants obtained from these potentials but was essential for correctly calculating the zero-field mobility, especially at low *T*.

III. Results and Discussion

A. Spectroscopic Constants

The RCCSD(T)/aV∞Z potentials are shown in Figure 1 for $C^+(^2P)$-He and in Figure 2 for $C^+(^4P)$-He, and the values are also included as Supplementary Material. The spectroscopic constants obtained from the interaction potentials are presented in Table 1 for $^{12}C^+$ and in Table 2 for $^{13}C^+$. We shall discuss the results for each C^+ state in turn, comparing with previous work where available, concentrating on the $^{12}C^+$ results, since previously-reported results are only available for this isotope. In addition, Tables 3 and 4 give the bound vibrational levels for the doublet and quartet states, respectively; only the levels from the spin-orbit states are given since these are the ones that would be observed experimentally.

i. $C^+(^2P)$ with helium

The ground state of C^+ has the electronic configuration $1s^22s^22p^1$, giving rise to a ^2P state. For $C^+(^2P)$, as shown previously,[11] the $^2\Pi$ state is lower in energy than the $^2\Sigma^+$ one. This ordering is as expected since the unpaired electron can be located in the $2p_z$ orbital, giving rise to the $^2\Sigma^+$ diatomic state, or in the $2p_{x,y}$ orbitals, giving rise to the $^2\Pi$ one. The former is expected to be more weakly bound, and higher in energy, owing to electron repulsion with the He atom; while the latter will be more strongly bound, since the 2p electron is located out of plane, and the He will be able to interact more with the exposed carbon dicationic core.

Our calculated $^2P_{3/2} - {}^2P_{1/2}$ spin-orbit splitting is 61.2 cm^{-1}, compared to the experimental value[9] of 63.4 cm^{-1}. The $^2\Pi_{1/2}$ state is lower in energy than the $^2\Pi_{3/2}$ state, in line with expectations for a less-than-half-filled orbital subshell.

We highlight that the spectroscopic constants for the $^2\Pi_{3/2}$ state are almost identical to those for the non-SO $^2\Pi$ state (see Table 1) as would be expected, since there is no other $\Omega = {}^3/_2$ state with which it can interact in this three-state picture. On the other hand, the $^2\Pi_{1/2}$ state can interact with the $^2\Sigma_{1/2}^+$

one, and this is found to lead to notably different spectroscopic constants for the two resultant $\Omega = {}^1/_2$ levels compared to the original (non-SO) terms, especially for the dissociation energies. (Recall that, despite this small interaction, we shall refer to the interacting states with the same designations as the non-interacting ones.) It can be seen that D_e, ω_e and k decrease upon inclusion of SO-splitting from $^2\Pi$ to $^2\Pi_{1/2}$, which correlates with the increase of these quantities for the $^2\Sigma_{1/2}{}^+$ state compared to the $^2\Sigma^+$ state. These changes are in line with the forms of the interaction potentials, shown in Figure 1. Except for D_e, the spectroscopic parameters for the $^2\Pi_{1/2}$ state are very close to those for the $^2\Pi$ one, since the mixing with the $^2\Sigma_{1/2}{}^+$ state is small close to the minimum of the $^2\Pi_{1/2}$ curve owing to the large energetic separation. The curves are energetically much closer in the region of the minimum of the $^2\Sigma_{1/2}{}^+$ curve and so more mixing occurs, and hence we see the spectroscopic parameters for the $^2\Sigma^+$ state being perturbed more than for the $^2\Pi_{1/2}$ one. These changes represent changes in the shape of the $^2\Sigma_{1/2}{}^+$ potential relative to the $^2\Sigma^+$ one. We do not see such changes in shape for the $^2\Pi_{3/2}$ level since, as mentioned above, there are no levels with which it can interact in the present three-state model and so it is unperturbed; any very small changes arise from numerical rounding in the spin-orbit diagonalization procedure.

In comparison to previous work (see Table 1, where we have only included results from correlated methods), for the $^2\Pi$ state we see reasonably good agreement of the equilibrium internuclear separation with all of the MP2, MP4(SDQ), QCISD(T) and CCSD(T)/cc-pVQZ calculations. The best agreement, however, is with the recent MRCI/d-aug-cc-pVQZ calculations of Matoba *et al.*,[19] and this confirms that the single-reference RCCSD(T) method employed here is adequate. Similarly good agreement is seen with the range of previous values for the dissociation energy. It is interesting to note that the agreement with the CCSD(T)/cc-pVQZ D_0 value from Hughes and von Nagy-Felsobuki[18] is not as good as the corresponding aug-cc-pVTZ value from that work, suggesting that diffuse functions are important. Indeed, if one uses the ratio of the cc-pVTZ and aug-cc-pVTZ D_0 values from ref. 18 to scale the cc-pVQZ one, an "aug-cc-pVQZ" value of 391 cm^{-1} is obtained – very close to the present value. The reason for this cc-pVQZ discrepancy appears to lie in the vibrational frequency calculated in ref. 18, which is significantly higher than the present value (see Table 1).

For the $^2\Sigma^+$ state, only two previous reports of the equilibrium internuclear separation and dissociation energy have been reported. The MP4(SDQ) values of Grice *et al.*[16] are in reasonable agreement with the present ones, while the MRCI values from Matoba *et al.*[19] are in excellent agreement with the present values.

ii. $C^+(^4P)$ with helium

The $C^+(^4P)$ state arises from a 2p ← 2s excitation, leading to a $1s^22s^12p^2$ configuration. Upon interaction with helium, in the absence of spin-orbit coupling, the degeneracy is lifted and $^4\Pi$ and $^4\Sigma^-$ states result. In the former case, one of the two electrons in the 2p orbital is located in the $2p_{x,y}$ orbitals, with the other in the $2p_z$; in the $^4\Sigma^-$ state, both 2p electrons are located in the $2p_{x,y}$ orbitals. As a consequence, we expect more electron repulsion with the He atom for the $^4\Pi$ term than for the $^4\Sigma^-$ term. Consistent with this, for $C^+(^4P)$ interacting with helium, the $^4\Sigma^-$ state was found to be lower in energy than the $^4\Pi$ state, as was shown previously.[16] Indeed, the magnitude of the binding energy of the helium atom in the $^4\Sigma^-$ state is quite remarkable. We note here that the $^4\Sigma^-$ state, as well as having both 2p electrons perpendicular to the internuclear axis, also has one fewer 2s electron than the $^2\Pi$ state; as such, the binding energy of the helium atom would indeed be expected to be significantly greater, as is shown in Table 1, as a result of its increased "view" of the dicationic core.

Since these states have quartet spin multiplicity, one more spin-orbit component arises here than was the case for $C^+(^2P_J)$ interacting with helium. The spin-orbit splittings for $^4P_{1/2} - {}^4P_{3/2} - {}^4P_{5/2}$ have been calculated to be 17.3 and 46.0 cm^{-1}, which compare well to the experimental values[9] of 22.0 and 50.3 cm^{-1}. The interaction potentials for all of these quartet SO states, as well as the non-SO states, are shown in Figure 2. For the $\Omega = {}^1/_2$ and $\Omega = {}^3/_2$ SO states arising from the $^4\Sigma^-$ term, we observe almost identical spectroscopic constants, since at the position of these minima the curves are significantly energetically separated from the like-Ω $^4\Pi$ curves; as such, the constants are extremely close to each other and those for the non-SO $^4\Sigma^-$ state. The minima of the $^4\Sigma_{1/2}^-$ and $^4\Sigma_{3/2}^-$ states are found to be degenerate, both because near their minimum they are too far away to interact with like-Ω states from the $^4\Pi$ manifold, and also since there is no spin-orbit coupling between them. (They would be split a small amount by spin-spin coupling, in reality, but that is not included here.)

For all four of the $^4\Pi_\Omega$ states the R_e values are very similar, and very close to the $^4\Pi$ value. The other spectroscopic constants show more significant differences, however, with all of the dissociation energies, harmonic vibrational frequencies and force constants being greater than for the $^4\Pi$ state, with the exception of those for the $^4\Pi_{5/2}$ state which are indistinguishable from those of the non-SO term. The latter is expected, since there is no other $\Omega = 5/2$ state with which it can interact. The largest changes are observed for the $^4\Pi_{1/2}$ state where D_e, ω_e, k and $\omega_e x_e$ demonstrate significant changes. We note that the variations in the spectroscopic parameters for the $^4\Pi_\Omega$ SO states are in contrast to those from $^4\Sigma_\Omega^-$ where almost no variation is seen. We postulate that this is due to the significant depth of the $^4\Sigma^-$ potential compared to the much shallower $^4\Pi$ one, which leads to the minimum of the $^4\Pi_\Omega$ curves being energetically close to the $^4\Sigma_\Omega^-$ curves in this region. The ordering of the $^4\Pi_\Omega$ states

(energetically from lowest to highest, and using signed values for Ω = 1/2) is Ω = -1/2, 1/2, 3/2 and 5/2. Thus, using the non-crossing rule we can see which spin-orbit states correlate to which atomic asymptote, with all involving He($^1S_0$). The $^4\Sigma_{1/2}^-$ state correlates to $C^+(^4P_{1/2})$; $^4\Sigma_{3/2}^-$ and $^4\Pi_{-1/2}$ correlate to $C^+(^4P_{3/2})$; and $^4\Pi_{5/2}$, $^4\Pi_{3/2}$ and $^4\Pi_{1/2}$ correlate to $C^+(^4P_{5/2})$. (Recall that states with the same-Ω value will be mixed to a small extent.)

With regard to previous work that did not include spin-orbit coupling, again there is very good agreement with the internuclear separation for the $^4\Sigma^-$ term; indeed, this is notably better than was observed for the $^2\Pi$ term. It has been noted by previous authors[18] that electron correlation is likely more important in the system with the larger equilibrium separation. The calculations of Grice *et al.*[16] show reasonably good agreement for the $^4\Sigma^-$ internuclear separation, but only fair agreement for the D_e value; with regard to the $^4\Pi$ state, in both cases the agreement is good. Reasonable agreement is also seen with the results of Hughes and von Nagy-Felsobuki[18] and also with their ω_e value, in contrast to the poorer agreement that was observed for the $^2\Pi$ state. In contrast, we note markedly poorer agreement with their cc-pVQZ D_0 value (11501 cm^{-1}) than the better agreement seen with their aug-cc-pVTZ value (9929 cm^{-1}); this seems largely to be due to the diffuse functions as the same marked effect is seen between the cc-pVTZ and aug-cc-pVTZ results in ref. 18. Again we can estimate the aug-cc-pVQZ value from the corresponding triple-ζ ratio, giving a value of 10306 cm^{-1}, which is in excellent agreement with the present value.

As was the case for the $C^+(^2P)$-He spectroscopic constants, we see very good agreement for both the $^4\Sigma^-$ and $^4\Pi$ states with the calculated internuclear separations and D_e values from the MRCI calculations of Matoba *et al.*[19]

B. Transport coefficients

i. $C^+(^2P)$ with helium

In the present work, ion mobilities and diffusion coefficients have been calculated from both the non-SO and the SO potentials arising from the lowest doublet and quartet states of C^+ interacting with helium. These are computed over a wide range of E/n_0 and at a variety of temperatures, including temperatures at which experimental data have been taken. Although ground, statistical and excited state weightings were used for zero-field and field-dependent calculations, only the values that can be compared to experiment are presented here; the full dataset is available in the Toulouse database.[40]

Cross-sections were calculated from each potential curve, and then various weightings of these were employed in generating the transport data to compare with experiment, since the actual ionic state

populations are not definitively known owing to: the ion production method; uncertainty regarding thermalization; injection effects; and the effect of the collisions during the ion drift region. For the doublet curves, the weightings chosen were those of the ground state (100% $^2\Pi$ or 100% $^2\Pi_{1/2}$ cross-sections), the excited state (100% $^2\Sigma^+$ or a 1:1 weighting of the $^2\Pi_{3/2}$ and $^2\Sigma_{1/2}{}^+$ cross-sections) and a statistical state (2:1 weighting of $^2\Pi$ and $^2\Sigma^+$ or a 1:1:1 weighting of $^2\Pi_{1/2}$, $^2\Pi_{3/2}$, $^2\Sigma_{1/2}{}^+$ cross-sections).

To avoid cluttered figures, we have plotted the different mobilities as follows. In Figure 3 we show three non-SO mobility curves: from the $^2\Pi$ and $^2\Sigma^+$ cross-sections individually, as well as from a statistical (2:1) mix of these; only the latter makes physical sense for random orientation collisions, corresponding to the ^2P state. For comparison, we also show the mobilities obtained from a statistical (1:1:1) mix of the $^2\Pi_{1/2}$, $^2\Pi_{3/2}$ and $^2\Sigma_{1/2}{}^+$ cross sections (corresponding to a statistical mix of $^2P_{1/2}$ and $^2P_{3/2}$ states) and also the smoothed data[22] from Dotan *et al.*[21] It is clear that the calculated statistical results are in closest agreement with the experimental data; however, with the size of the cited error bars, it is not possible to decide between the spin-orbit and non-spin-orbit results, even though we would expect the former to be the more reliable. In Figure 4 we show all available mobility data at room temperature, as well as the results from the individual spin-orbit curves and the statistical spin-orbit curve (also shown in Figure 3). It is clear that, particularly given the size of the various error bars, the experimental data are essentially in agreement across the whole range of E/n_0. Also clear is that the best match through the whole range is with the statistical mix of SO states with just the odd experimental point falling off this curve, within the given error bars.

To numerically compare the calculated and experimental mobilities, we calculated the dimensionless statistical quantities, δ and χ, which are defined in ref. 36. The quantity, δ, is a measure of the relative difference between the experimental and calculated values compared to the combined errors, and χ is a measure of the relative standard deviation compared to the sum of the squared error estimates. If $|\delta|$ is < 1, there is substantial agreement between the two sets of values (and the converse is true). If χ is about the same value of $|\delta|$, the agreement is about the same over the data set and there is little scatter, while if it substantially larger, then one of those two factors is not true.

Overall, we conclude that the mobilities indicate that statistical populations of the two ^2P_J components were present in the experiments. C^+ was created in these experiments by charge transfer or electron impact ionization, followed by thermalization to ~300 K. The Boltzmann population of the two spin-orbit states at 300 K may be calculated to be 1.00:0.37 for $^2P_{1/2}$:$^2P_{3/2}$, so one might expect different nascent populations. However, the ion mobility measurements are carried out in a flow of helium, and as noted by Twiddy *et al.*[24] *J*-changing collisions (calculated[8] to have a rate of ~ 10^{-10} molecule^{-1} cm^3 s^{-1} at 150 K and expected to be significantly faster at 300 K) will scramble any nascent population

differences. Coupled with the random orientation of the C^+/He collisions, this is consistent with our observation that a statistical mix of the spin-orbit cross sections gives excellent agreement with experiment. The fact that the non-SO statistical state also gives good agreement, while the other non-SO states do not is again a result of the random orientations of the C^+/He collisions.

Below 100 Td, the data of Peska[23] are well represented by the calculated statistical data, but visually there is some deviation to higher E/n_0 values. Over the whole data set, this is not a statistically significant deviation (Table 5), but it may point to more significant errors in the experiment at these larger values. We also note that the room temperature data reported by Thomas *et al.*[20] is generally in good agreement with the present data and with previous results, but the data points at the lowest values of E/n_0 (and the apparent trend here) appear to be anomalous. Their diffusion data (see Table 5) is in marked disagreement with the present calculated results and we conclude it is unreliable.

We also note that our results indicate that the uncertainties attributed to the experimental data in refs. 21, 23 and 24 are perhaps somewhat pessimistic, particularly for E/n_0 values below 100 Td. We note that the magnitude of the experimental errors, coupled with the very small difference between the statistical SO and non-SO calculated values, implies we are unable to discriminate between these; we would, however, expect the SO results to be the more reliable. The conclusion that a statistical mix of states is more representative is (indirectly) in agreement with the conclusions of Grice *et al.*,[16] who calculated mobilities from non-SO interaction potentials, obtained using the MP4(SDQ)/6-311+G(3df,3pd) approach. They found that a 2:1 weighting of the $^2\Pi$:$^2\Sigma^+$ cross sections gave reasonable agreement with experiment, while the individual results for the $^2\Pi$ and $^2\Sigma^+$ states were in poor agreement; again, a feature of the random C^+/He collisional orientations.

We will now consider the more recent low temperature mobility results of Matoba *et al.*[19] Figure 5 and Table 5 shows a comparison of their experimental ^2P data to our predicted mobilities using various weightings for the calculated mobilities at 77 K. These suggest that for E/n_0 in the range 10–100 Td, the statistical mix gives the best agreement, passing smoothly through the mobility maximum, while at $E/n_0 < 10$ the experimental results veer towards those of $C^+(^2P_{1/2})$. Although this could point to an experimental issue, this would also be in line with the significantly greater Boltzmann population of the lower state at 77 K (population ratio 1.00: 0.15, assuming complete thermalization), consistent with lower-energy collisions at lower E/n_0 values which would not be expected to lead to efficient spin-orbit state change, and so maintaining the nascent Boltzmann populations.

When we compare our calculated mobilities with Matoba *et al.*'s 4.3 K experimental data,[19] Figure 6 and Table 5, little agreement is seen for any of the results, although there is perhaps an argument that the data are closest to that of the $^2P_{1/2}$ state for moderate E/n_0. We believe that the disagreement in the

high E/n_0 regions is partly due to the small uncertainties cited, as evinced by the correct shape of the experimental mobility curve above about 50 Td, but there are other issues that are not so easy to ascribe.

First, the significant "mobility minimum" seen in the experimental data at ~ 10 Td is extremely unusual and is not present in the calculated values. Such results have often been found in the very low temperature work of Kaneko, Tanuma and colleagues[41,42,43] as well as the results in ref. 19. For molecular ions, it has been argued[44,45] that it occurs because of a Feshbach-type resonance; however, this explanation cannot account for the same behaviour being observed in atomic ion-atom systems. It has been argued[46] that calculations like the ones described here might show a mobility minimum if the cross sections were computed quantum-mechanically, rather than by using the classical-mechnical techniques inherent in program PC. However, a careful, exhaustive study[47] found this to not be the case for Ar^+ in He, so it seems unlikely that it could be true here.

Secondly, it was found in 2000[48] that there are no mobility minima for He^+ and Ar^+ ions in He when proper consideration is given to the thermal transpiration effects. These occur when a pipe is used to connect a very low temperature drift tube with a room temperature manometer. Unfortunately, it was not reported in ref. 19 whether or how thermal transpiration effects were taken into account.

Thirdly, we note that the calculated mobilities at 77 K and 4.3 K are very close to each other at high E/n_0, and only deviate at low E/n_0, and even then only to a small extent. Since there will be little difference between the regions of the interaction potentials sampled during such low temperature collisions, this is in line with expectations; in contrast, the experimental data show significant differences between the 77 and 4.3 K data over all E/n_0 regions.

We have noted above that Matoba *et al.*[19] calculated MRCI interaction curves for $C^+(^2P)$ interacting with $He(^1S)$, and very good agreement is obtained for R_e and D_e with the present potentials. From their (non-SO) MRCI potentials, Matoba *et al.*[19] calculated mobilities using the first approximation of the two-temperature kinetic theory (which can be wrong by as much as 10%). They concluded that neither the $^2\Pi$ nor $^2\Sigma^+$ potentials gave good agreement with experiment, but that the weighted average did (which would be consistent with random orientation collisions); however, they did not specify whether they used a 1:1 weighting of the $^2\Pi$ and $^2\Sigma^+$ cross sections, or the statistical weighting of 2:1 and apparently the mobilities were only calculated at a single (unspecified) temperature. We also note that their calculated mobilities are not in such good agreement with ours (compare our Figures 5 and 6 with their Figure 5), particularly at high E/n_0, but the similar behaviour is observed at low E/n_0, i.e. that the experimental data drop below the calculated statistical mobilities and approach those of the $^2P_{1/2}$ ($^2\Pi$ for Matoba *et al.*) state. Finally, a small mobility minimum appears in Matoba *et al.*'s calculated data from the $^2\Sigma^+$ state, but this is not present in the weighted average they report. We thus

conclude that the 4.3 K data of Matoba *et al.*[19] are unreliable. This could arise from incomplete thermalization (at 4.3 K, the Boltzmann population of the $^2P_{3/2}$ state is almost zero), but this would not explain the significant mobility minimum. One possible explanation is thermal transpiration, as mentioned above. Another is complexation of C^+ with He during the drift region followed by rapid collisional break up. This would lead to a slight slowing of the passage of C^+ down the drift tube, and hence to lower mobilities. The significance of this process would depend on E/n_0 as there would need to be a balance of there being a high enough collisional frequency to form the complexes, but also enough energy for a significant number to dissociate (collisionally, or via unimolecular decay) rapidly, so that they arrived at close to the correct time of flight. Matoba *et al.*[19] present time-of-flight spectra in Figure 1 of their work, and broadening of the spectral features does appear to occur at the E/n_0 values shown, although these are not as low as 10 Td. Although several pressures were used at both 4.3 and 77 K, with no significant changes detected in the mobilities, the pressures used, particularly at 4.3 K, do not appear to have differed enough to rule out the formation of ion-neutral clusters as an explanation for the mobility minimum.

ii. $C^+(^4P)$ with helium

With regard to the $C^+(^4P)$ state mobility data, there are only the studies of Twiddy *et al.*[24] at room temperature and Matoba *et al.*[19] at 77 and 4.3 K to which we can compare. A smoothed version of the Twiddy *et al.*[24] data has been compiled in the work of Viehland and Mason.[49] The room temperature experimental data are compared to our calculated results in Figure 7 and Table 6, which shows the results for each of the three ^4P_J states, with the mobilities for $^4P_{1/2}$ state coming from the $^4\Sigma_{1/2}^-$ curve, for the $^4P_{3/2}$ state from a 1:1 mix of the $^4\Sigma_{3/2}^-$ and $^4\Pi_{(-1/2)}$ curves, and for the $^4P_{5/2}$ from a 1:1:1 mix of the $^4\Pi_{1/2,}$ $^4\Pi_{3/2}$ and $^4\Pi_{5/2}$ curves, in line with the curves that correlate to the different atomic asymptotes. Additionally, a statistical (equal) weighting of the six diatomic SO states is shown. It may be seen that only the statistical results are in good agreement with the experimental results of Twiddy *et al.*[24] indicating that the data are indeed for $C^+(^4P)$ ions, as also confirmed by Grice *et al.*[16] As such, as was seen for $C^+(^2P)$, we conclude a statistical mixture of the SO states is appropriate at room temperature, owing to the random nature of the collisions and, it is assumed, efficient spin-orbit-changing collisions; notwithstanding the thermalized nascent Boltzmann population ratios of 1.00: 0.45: 0.26 for $^4P_{1/2}$: $^4P_{3/2}$: $^4P_{5/2}$. We note that although the agreement between the Grice *et al.*[16] calculated values and Twiddy *et al.*'s experimental data may seem better by eye than the present work (see Figure 2 of Grice *et al.*'s paper) they both agree within the experimental uncertainties. The present results should be the more reliable, given the inclusion of spin-orbit coupling and the higher level of theory employed.

Comparisons of our calculated mobilities to the 77 K and 4.3 K $C^+(^4P)$ mobilities of Matoba *et al.*[19] are given in Figures 8 and 9, and Table 6. Owing to the small experimental uncertainties given, the agreement with the calculated values is poor, but the trend in the values is correct and perhaps points to the uncertainties being optimistic. If this were the case, then the statistical values seem most likely to describe the data: although the calculated data for the $^4P_{3/2}$ state could be argued also to fit, there is no reason for this particular spin-orbit state to be preferentially populated. We note that, owing to experimental difficulties in deconvoluting the ^4P mobility feature from the ^2P one, data at low E/n_0 were not obtained, and hence whether the movement of the mobility data towards the lowest SO state occurs or not is unestablished. At 4.3 K, again the experimental uncertainties seem too small; excluding the $^4P_{3/2}$ state as being unlikely, it is difficult to say with any certainty what calculated curves fit the experimental data the best, although the statistical curve seems the most likely, albeit that the agreement is poor. Again, as noted above, it may be that complexation at these low temperatures occurs, leading to lower observed mobilities.

It is interesting to note that there is a small mobility minimum at 4.3 K in the calculated values from the statistical combination of non-SO states for quartet C^+, but this is not present in the values from the statistical combination of SO states, although the data are close elsewhere. This minimum is much smaller than the experimental minimum at 4.3 K for doublet C^+, and our minimum has been traced to small differences in the potentials at around 5 Å. This shows the great sensitivity of mobility values to even very subtle changes in interatomic potentials.

IV Concluding Remarks

We have calculated high-level interaction potentials for $C^+(^2P)$ and $C^+(^4P)$ interacting with He, both with and without the inclusion of spin-orbit coupling. Additionally, we present spectroscopic constants obtained using these potentials and show that these are mostly in agreement with available published data. The present results are, however, more complete and also are expected to be the most reliable. Comparing the curves with and without spin-orbit coupling, we find that the perturbation to the spectroscopic constants obtained is small, but more significant for the upper states in each case, $^2\Sigma^+$ and $^4\Pi$, owing both to their more-weakly-bound nature and the energetic proximity of the two non-SO curves at internuclear separations close to the minima of the respective upper states.

We have also calculated transport data for both sets of ions, $C^+(^2P)$ and $C^+(^4P)$, with the focus on ion mobilities, for which there is the most experimental data. For $C^+(^2P)$, at ~ 300 K we were able to show that the data of Thomas *et al.*[20] are unreliable for diffusion coefficients, while there is generally good agreement with the experimental mobility data of Thomas *et al.*,[20] Dotan *et al.*,[21] Peska[23] and Twiddy

et al.,[24] as well as with the calculated values of Grice *et al.*[16] It was shown that a statistical mix of the ionic (spin-orbit) states gave the best agreement with experiment (a similar agreement was reached by ourselves in previous work on the open shell O^- and S^- ions in He[50,51]); with the SO and non-SO results giving very similar values. This was notwithstanding the expected difference in nascent spin-orbit populations, and is a result of rapid *J*-changing collisions at this temperature as well as the random orientations of the collisions. At the lower temperature of 77 K, comparison between the experimental data of Matoba *et al.*[19] and the calculated values suggested that at high E/n_0 a statistical picture of the states matches the experimental data best, while at low E/n_0 there was significant deviation from this towards the results of the lower $^2P_{1/2}$ state, in line with lower collision energies and the higher population of this state at this lower temperature. We found that there was stark disagreement between the calculated values and experimental data for high and low E/n_0 values at 4.3 K, and suggest that this could be the result of increased likelihood of short-lived complexation between C^+ and He, but may also be due to thermal transpiration effects or experimental difficulties in extracting data from overlapping mass peaks in the arrival spectra. There was some evidence at moderate E/n_0 values that the calculated $^2P_{1/2}$ results fitted the data best here.

For $C^+(^4P)$, the data are more limited: good agreement was seen with the experimental ~ 300 K data of Twiddy *et al.*[24] and the calculated values of Grice *et al.*[16] For the lower 77 K and 4.3 K temperatures, the data of Matoba *et al.*[19] were again limited, but the agreement with the calculated values was not good and seems partly attributable to optimistic cited experiment uncertainties; in particular, there were cited difficulties with overlapping features in the arrival spectra for the ^4P state. In addition, we note that there was the possibility of complexation of C^+ with He.

The present spectroscopic results could prove useful for trying to detect the C^+-He complex in the interstellar medium, as suggested by Harrison *et al.*[7] although whether sufficient quantities would be present is not clear, with direct formation of the complex requiring three-body stabilization by another atom/molecule or surface; also, ligand exchange is also unlikely owing to the low binding energy. We note the importance of accounting for ion mobilities in determining accurate rate coefficients,[24] particularly for slow reactions; the present calculated mobilities at a range of temperatures will clearly be useful in such investigations.

Finally, we highlight that our calculated mobilities suggest that, in principle, it could be possible to separate different atomic spin-orbit states on the basis of their mobilities. However, we have also shown that for experiments carried out at room temperature, spin-orbit-changing collision lead to complete scrambling of this, and mobilities calculated with statistical mixes of all contributing states need to be used to obtain agreement with experiment. There is, however, some indication from the 77 K data from Matoba *et al.*, notwithstanding the caveats noted above regarding the reliability of these

data, that low temperatures and/or low collision energy may make such separation possible. For spin-orbit states with larger energetic separations than here, this may be more feasible and is something we shall consider in work on the heavier Group 14 cations.

Acknowledgements

TGW, WDT and RLT are grateful for the provision of computing time by the EPSRC under the auspices of the NSCCS, and are also grateful for access to the University of Nottingham High Performance Computing Facility. The EPSRC are thanked for the provision of a studentship to W.D.T.

Figure Captions

These are located above each figure, below.

Table 1: Spectroscopic constants for $^{12}C^{+}(^{2}P_J)$-He and $^{12}C^{+}(^{4}P_J)$-He

State	R_e / Å	D_e / cm^{-1}	D_0 / cm^{-1}	ω_e / cm^{-1}	$\omega_e x_e$ / cm^{-1}	k / N m^{-1}	B_e / cm^{-1}	Reference
$^{2}\Pi_{1/2}$	2.201	456.3	368.5	185.5	19.67	6.083	1.159	This work
$^{2}\Pi_{3/2}$	2.200	476.2	388.0	186.0	19.07	6.120	1.160	This work
$^{2}\Pi$ (no SO)	2.200	476.1	387.9	186.0	19.07	6.120	1.160	This work
	2.406	385	315	142				[a]
	2.504							[b]
	2.233	481(542)[c]	359(420)[c]	243.7				[c]
	2.329	406						[d]
	2.21	468						[e]
$^{2}\Sigma_{1/2}^{+}$	2.946 2.978 2.99	135.5 147 122	93.9	92.45	18.43	1.512	0.647	This work [d] [e]
$^{2}\Sigma^{+}$ (no SO)	2.968	121.8	83.3	85.88	17.83	1.304	0.638	This work
$^{4}\Sigma_{1/2}^{-}$	1.153	10981.7	10286.6	1405.6	30.95	349.4	4.225	This work
$^{4}\Sigma_{3/2}^{-}$	1.153	10998.9	10303.8	1405.7	30.95	349.4	4.225	This work
$^{4}\Sigma^{-}$ (no SO)	1.153	11010.4	10315.3	1405.7	30.95	349.4	4.225	This work
	1.168	10248	9653	1196				[a]
	1.177							[b]
	1.156	10579 (12151)[c]	9929 (11501)[c]	1334.5				[c]
	1.158	10254						[d]
	1.16	10691						[e]
$^{4}\Pi_{(-1/2)}$	2.747	168.6	122.5	100.9	17.12	1.800	0.744	This work
$^{4}\Pi_{1/2}$	2.745	185.5	138.2	102.3	15.35	1.850	0.745	This work
$^{4}\Pi_{3/2}$	2.747	174.4	128.1	100.9	16.49	1.800	0.744	This work
$^{4}\Pi_{5/2}$	2.750	163.7	118.3	99.48	17.34	1.750	0.743	This work
$^{4}\Pi$(no SO)	2.750	163.7	118.3	99.47	17.34	1.750	0.743	This work
	2.805	175						[d]
	2.78	159						[e]

[a] Frenking *et al.*,[15] geometries and vibrational frequencies were obtained with MP2/6-31G(d,p) while dissociation energies were obtained from MP4(SDTQ)/6-311G(2df,2pd)/ MP2/6-31G(d,p) single point energies.
[b] Jemmis *et al.*,[17] QCISD(T)/6-311G(MC)** – see ref. 17 for details of basis set.
[c] Hughes and Von Nagy-Felsobuki,[18] R_e and D_e values obtained with CCSD(T)/cc-pVQZ; D_e and D_0 values given are obtained with the aug-cc-pVTZ (cc-pVQZ) basis sets; the D_e value has been obtained from the D_0 value using the cc-pVQZ ω_e value.
[d] Grice *et al.*,[16] MP4SDQ/6-311+G(3df,3pd).
[e] Matoba *et al.*,[19] MCSCF/MRCI/d-aug-cc-pVQZ with 1s of C^+ frozen in MRCI

Table 2: Spectroscopic constants for $^{13}C^{+}(^{2}P_J)$-He and $^{13}C^{+}(^{4}P_J)$-He

State	R_e / Å	D_e / cm^{-1}	D_0 / cm^{-1}	ω_e / cm^{-1}	$\omega_e x_e$ / cm^{-1}	k / N m^{-1}	B_e / cm^{-1}
$^{2}\Pi$ (no SO)	2.200	476.1	388.7	184.2	18.70	6.120	1.138
$^{2}\Pi_{1/2}$	2.201	456.3	369.3	183.7	19.28	6.083	1.137
$^{2}\Pi_{3/2}$	2.200	476.2	388.8	184.2	18.70	6.121	1.138
$^{2}\Sigma^{+}$ (no SO)	2.968	121.8	83.6	85.06	17.51	1.305	0.625
$^{2}\Sigma_{1/2}^{+}$	2.946	135.5	94.2	91.57	18.09	1.512	0.635
$^{4}\Sigma^{-}$ (no SO)	1.153	11010.4	10322.9	1390.1	29.91	348.5	4.143
$^{4}\Sigma_{1/2}^{-}$	1.153	10981.7	10294.1	1390.1	29.91	348.5	4.143
$^{4}\Sigma_{3/2}^{-}$	1.153	10998.9	10311.4	1390.1	29.91	348.5	4.143
$^{4}\Pi$(no SO)	2.750	163.7	118.7	98.5	17.02	1.750	0.728
$^{4}\Pi_{(-1/2)}$	2.747	168.6	122.9	99.9	16.80	1.800	0.730
$^{4}\Pi_{1/2}$	2.745	185.5	138.6	101.3	15.05	1.850	0.731
$^{4}\Pi_{3/2}$	2.747	174.4	128.5	99.9	16.18	1.800	0.730
$^{4}\Pi_{5/2}$	2.750	163.8	118.7	98.5	17.02	1.750	0.728

Table 3: Vibrational energy levels (cm^{-1}) for the three spin-orbit doublet states of $^{12}C^{+}$-He arising from the $^{12}C^{+}(^{2}P_J)$ + He($^{1}S_0$) asymptote. Also given is the energy at the minimum, E_{min}, for each case.
Energies are given with respect to each dissociation asymptote. Values for $^{13}C^{+}$-He states are given as Supplementary Material

v	$^{2}\Pi_{1/2}$	$^{2}\Pi_{3/2}$	$^{2}\Sigma_{1/2}^{+}$
E_{min}	-456.30	-476.21	-135.47
0	-368.48	-387.95	-93.85
1	-222.35	-240.06	-38.25
2	-117.77	-131.40	-12.02
3	-52.85	-60.86	-2.43
4	-18.90	-22.67	-0.17
5	-4.72	-6.06	

Table 4 : Vibrational energy levels (cm^{-1}) for the six spin-orbit quartet states of $^{12}C^{+}$-He arising from the $^{12}C^{+}(^{4}P_J)$ + He($^{1}S_0$) asymptote. Also given is the energy at the minimum, E_{min}, for each case.
Energies are given with respect to each dissociation asymptote. Values for $^{13}C^{+}$-He states are given as Supplementary Material

v	$^{4}\Sigma_{1/2}^{-}$	$^{4}\Sigma_{3/2}^{-}$	$^{4}\Pi_{-1/2}$	$^{4}\Pi_{1/2}$	$^{4}\Pi_{3/2}$	$^{4}\Pi_{5/2}$
E_{min}	-10981.68	-10998.93	-168.61	-185.46	-174.39	-163.75
0	-10286.59	-10303.84	-122.45	-138.16	-128.06	-118.35
1	-8942.84	-8960.09	-55.81	-66.58	-60.16	-53.55
2	-7654.14	-7671.39	-20.18	-25.43	-22.42	-19.16
3	-6447.63	-6464.88	-5.18	-7.11	-6.00	-4.83
4	-5339.59	-5356.84		-1.09		
5	-4337.79	-4355.03		-0.03		
6	-3445.41	-3462.64				
7	-2663.32	-2680.54				
8	-1991.11	-2008.32				
9	-1427.39	-1444.57				
10	-969.60	-986.72				
11	-613.53	-630.52				
12	-352.56	-369.16				
13	-177.33	-192.39				
14	-76.28	-86.44				
15	-28.10	-32.76				
16	-7.87	-9.62				

Table 5: Statistical comparison of calculated ion transport quantities to experimental data for $^{12}C^{+}(^{2}P_J)$.[a]

States	T / K	E/n_0 in Td (T)	N	δ	χ
K_0 Comparison with Ref. 20					
Statistical (non-SO)[b]	300	31–111	11	-0.09	0.95
$^2P_{3/2}$ [c]				0.55	1.08
$^2P_{1/2}$ [d]				-1.84	2.10
Statistical (SO)[e]				-0.16	1.00
K_0 Comparison with Ref. 22					
Statistical (non-SO)[b]	297	3.5–100.0	17	0.00	0.20
$^2P_{3/2}$ [c]				0.22	0.80
$^2P_{1/2}$ [d]				-0.85	1.80
Statistical (SO)[e]				-0.08	0.20
K_0 Comparison with Ref. 21					
Statistical (non-SO)[b]	297	3.5–100.0	31	0.08	0.20
$^2P_{3/2}$ [c]				0.74	1.00
$^2P_{1/2}$ [d]				-1.76	2.24
Statistical (SO)[e]				0.00	0.20
K_0 Comparison with Ref. 23					
Statistical (non-SO)[b]	300	10.0–170.0	43	-0.16	0.80
$^2P_{3/2}$ [c]				0.48	1.00
$^2P_{1/2}$ [d]				-2.05	2.57
Statistical (SO)[e]				-0.27	1.00
K_0 Comparison with Ref. 24					
Statistical (non-SO)[b]	297	7.3–113.7	14	0.21	0.30
$^2P_{3/2}$ [c]				0.93	1.10
$^2P_{1/2}$ [d]				-1.62	2.05
Statistical (SO)[e]				0.17	0.30
ND_L [f] Comparison with Ref. 20					
Statistical (non-SO)[b]	300	3.5–80.0	11	-4.45	4.57
$^2P_{3/2}$ [c]				-4.41	4.65
$^2P_{1/2}$ [d]				-4.49	4.57
Statistical (SO)[e]				-4.86	4.98

K_0 Comparison with Ref. 19					
Statistical (non-SO)[b]	77	2–65	21	-1.87	2.74
$^2P_{3/2}$ [c]				-2.11	4.66
$^2P_{1/2}$ [d]				-0.43	2.60
Statistical (SO)[e]				-1.69	2.35
K_0 Comparison with Ref. 19					
Statistical (non-SO)[b]	4.3	3–60	19	-3.22	3.63
$^2P_{3/2}$ [c]				-2.78	3.48
$^2P_{1/2}$ [d]				-3.01	3.34
Statistical (SO)[e]				-2.60	3.01

[a] See text regarding the statistical quantities δ and χ. *N* is the number of experimental data points in each case.
[b] These data correspond to $C^+(^2P)$ and arises from a 2:1 weighting of the $^2\Pi$ and $^2\Sigma^+$ results.
[c] These data correspond to $C^+(^2P_{3/2})$ and arise from a 1:1 weighting of the $^2\Pi_{3/2}$ and $^2\Sigma_{1/2}{}^+$ results.
[d] These data correspond to $C^+(^2P_{1/2})$ and arise from the $^2\Pi_{1/2}$ results.
[e] These data correspond to a statistical mix of $C^+(^2P_{1/2})$ and $C^+(^2P_{3/2})$ and correspond to a 1:1:1 weighting of the $^2P_{1/2}$, $^2\Pi_{3/2}$ and $^2\Sigma_{1/2}{}^+$ results.
[f] ND_L represents the longitudinal diffusion coefficient multiplied by the gas number density

Table 6: Statistical comparison of calculated ion transport quantities to experimental data for $^{12}C^{+}(^{4}P_J)$.[a]

States	T/K	E/n_0 in Td	N	δ	χ
K_0 Comparison with Ref. 24					
Statistical (non-SO)[b]	297	15–117	19	-0.65	0.67
$^{4}P_{5/2}$[c]				-3.53	3.55
$^{4}P_{3/2}$[d]				2.78	2.89
$^{4}P_{1/2}$[e]				5.18	5.23
Statistical (SO)[f]				-0.71	0.73
K_0 Comparison with Ref. 19					
Statistical (non-SO)[b]	77	32–60	7	-2.93	2.99
$^{4}P_{5/2}$[c]				-11.1	11.1
$^{4}P_{3/2}$[d]				2.78	2.89
$^{4}P_{1/2}$[e]				17.7	17.7
Statistical (SO)[f]				-3.18	3.23
K_0 Comparison with Ref. 19					
Statistical (non-SO)[b]	4.3	36–55	5	-2.22	2.24
$^{4}P_{5/2}$[c]				-7.99	-7.99
$^{4}P_{3/2}$[d]				0.55	0.69
$^{4}P_{1/2}$[e]				11.3	11.3
Statistical (SO)[f]				-2.33	2.35

[a] See text regarding the statistical quantities δ and χ. N is the number of experimental data points in each case.
[b] These data correspond to $C^{+}(^{4}P)$ and arises from a 2:1 weighting of the $^{4}\Pi$ and $^{4}\Sigma^{-}$ results.
[c] These data correspond to $C^{+}(^{4}P_{5/2})$ and arise from a 1:1:1 weighting of the $^{4}\Pi_{5/2}$, $^{4}\Pi_{3/2}$ and $^{4}\Pi_{1/2}$ results.
[d] These data correspond to $C^{+}(^{4}P_{3/2})$ and arise from a 1:1 weighting of the $^{4}\Sigma_{3/2}^{-}$ and $^{4}\Pi_{-1/2}$ results.
[e] These data correspond to $C^{+}(^{4}P_{1/2})$ and arise from the $^{4}\Sigma_{1/2}^{-}$ results.
[f] These correspond to a statistical mix of the SO states and arise from an equal weighting of the six SO states.

Figure 1: Interaction potentials for $C^+(^2P_J)$-He. The dashed lines show the non-SO potentials while the solid lines with markers show the SO potentials. Note that although these are interaction potentials, these have been shifted so that zero energy is defined as the non-SO asymptote, with the SO potentials split either side of this.

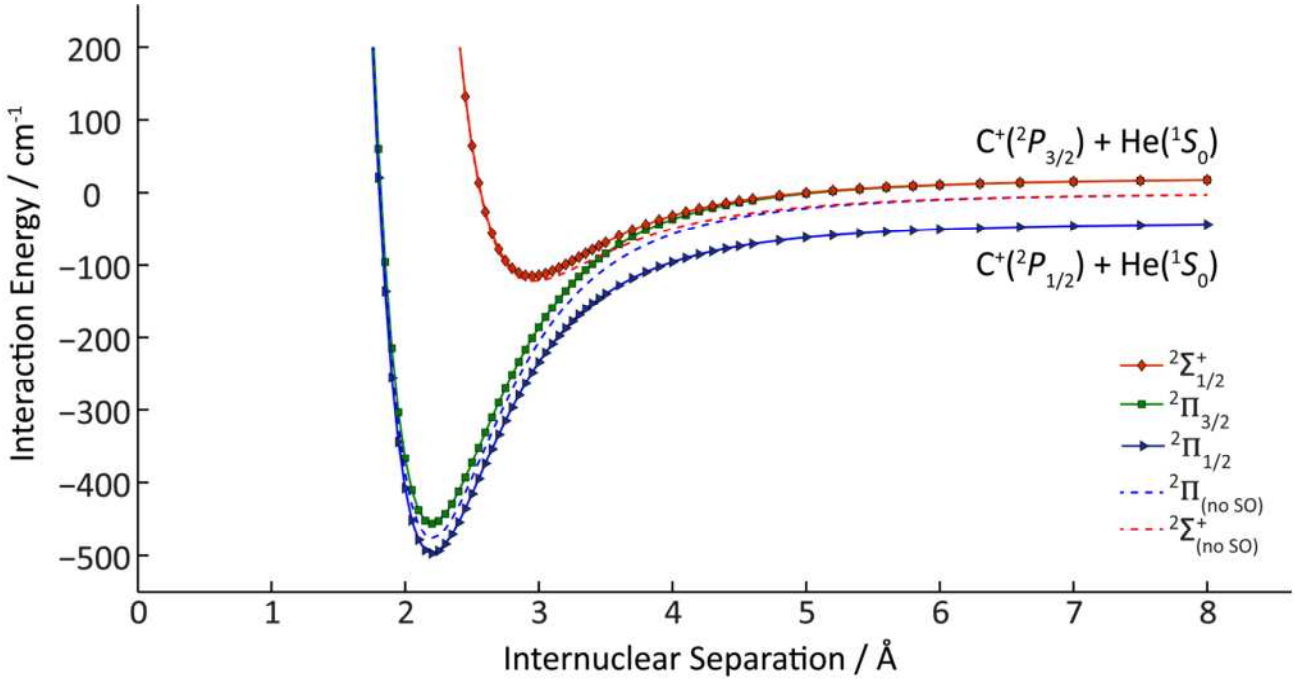

Figure 2: Interaction potentials for $C^+(^4P_J)$-He. The main figure shows an expanded view of the $^4\Pi_\Omega$ interaction potentials around their equilibrium internuclear separation and the inset shows the full interaction potentials for the non-SO $^4\Sigma^-$ and $^4\Pi$ states. (Only the non-SO potentials are shown in the inset, since the scale would render the difference between the SO and non-SO potentials impossible to see.)

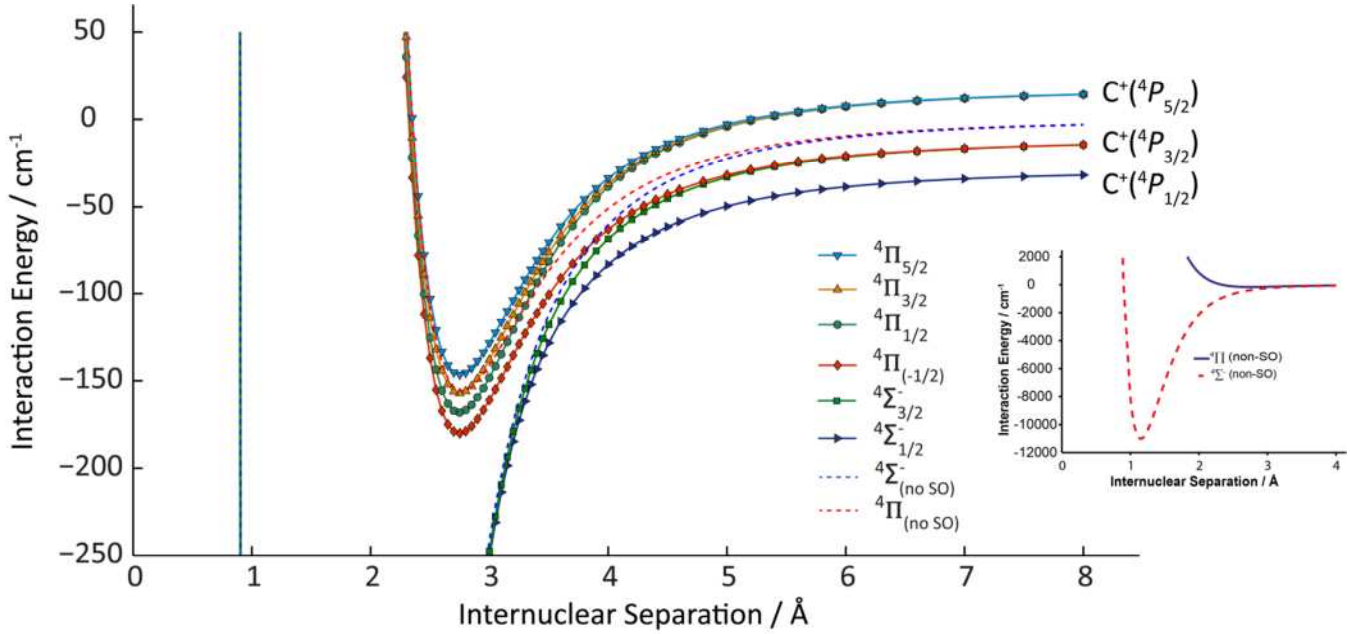

Figure 3: Comparison of the experimental and calculated $^{12}C^{+}(^{2}P)$ mobilities in helium at ~300 K, as a function of E/n_0 comparing the results for the $^{2}\Pi$ and $^{2}\Sigma^{+}$ states, a statistical (2:1) mix of these, and also a statistical mix of the SO states. (Further plots for the latter are shown in Figure 4.) The data points with error bars are the experimental results from Dotan *et al.*[21]

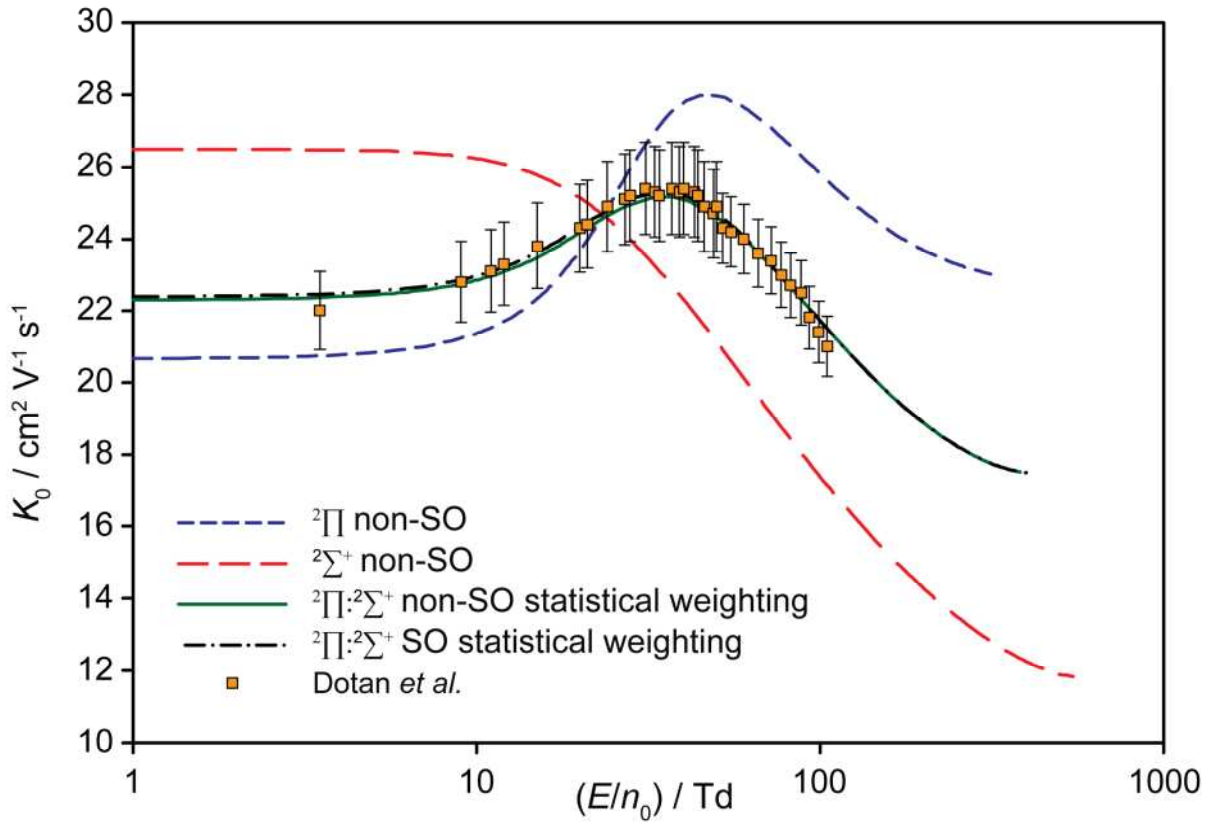

Figure 4: Comparison of the experimental and calculated $^{12}C^{+}(^{2}P_J)$ mobilities in helium at ~ 300 K, as a function of E/n_0. The points with error bars are the experimental values from: Thomas *et al.*[20], Dotan *et al.*,[21] Peska[23] and Twiddy *et al.*[24]

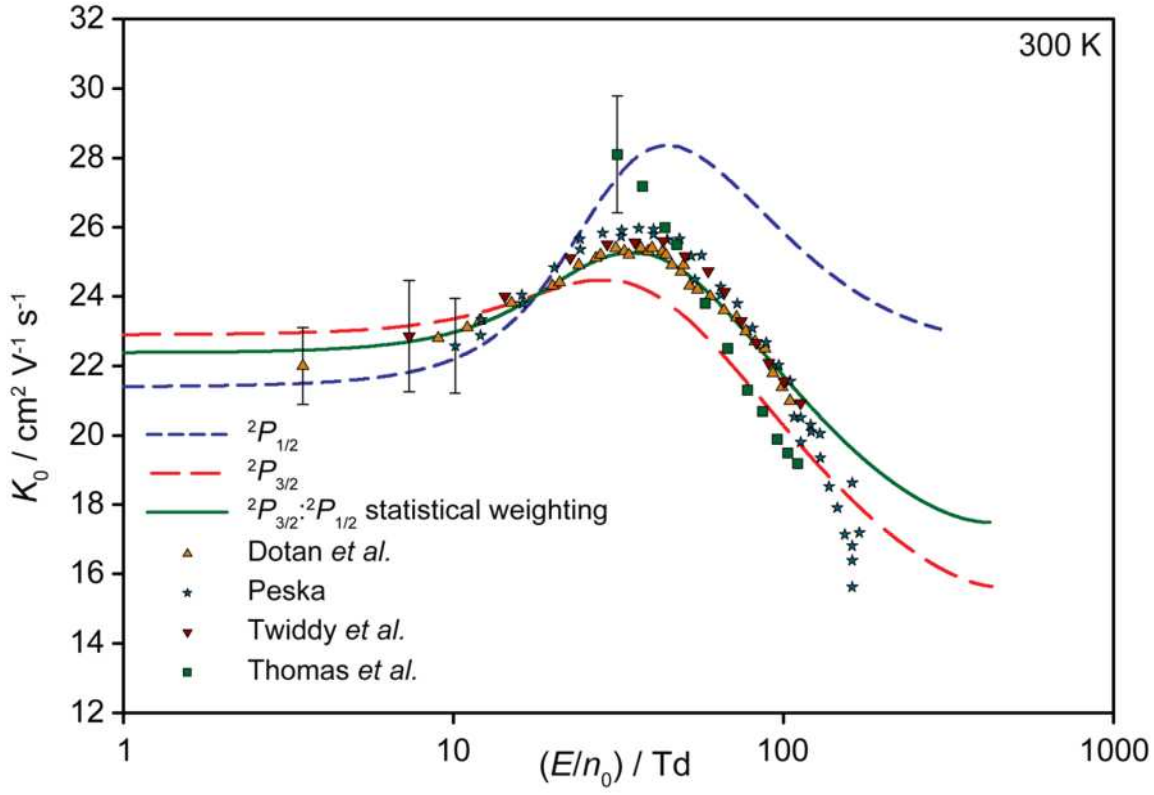

Figure 5: Comparison of the experimental and calculated $^{12}C^{+}(^{2}P_J)$ mobilities in helium at 77 K, as a function of E/n_0. The points with error bars are the experimental values from Matoba *et al.*[19]

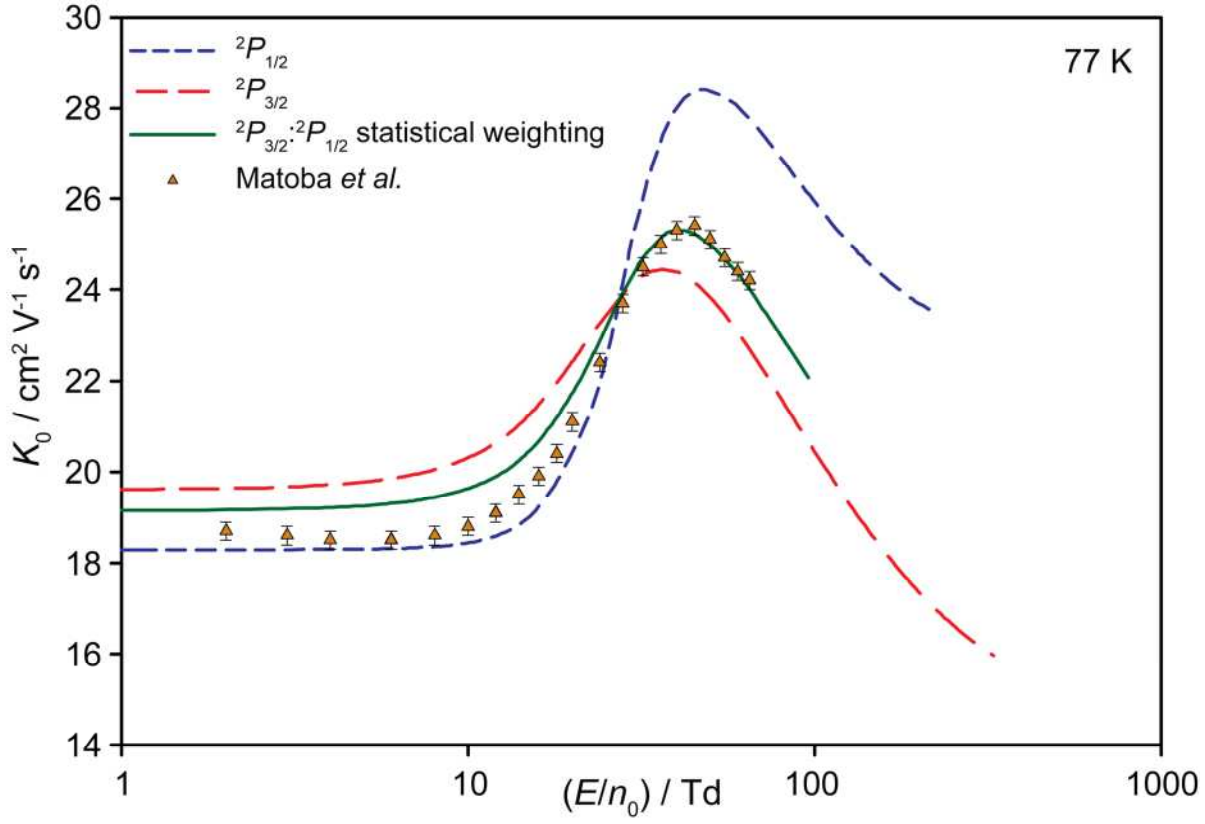

Figure 6: Comparison of the experimental and calculated $^{12}C^{+}(^{2}P_J)$ mobilities in helium at 4.3 K, as a function of E/n_0. The points with error bars are the experimental values from Matoba *et al.*[19]

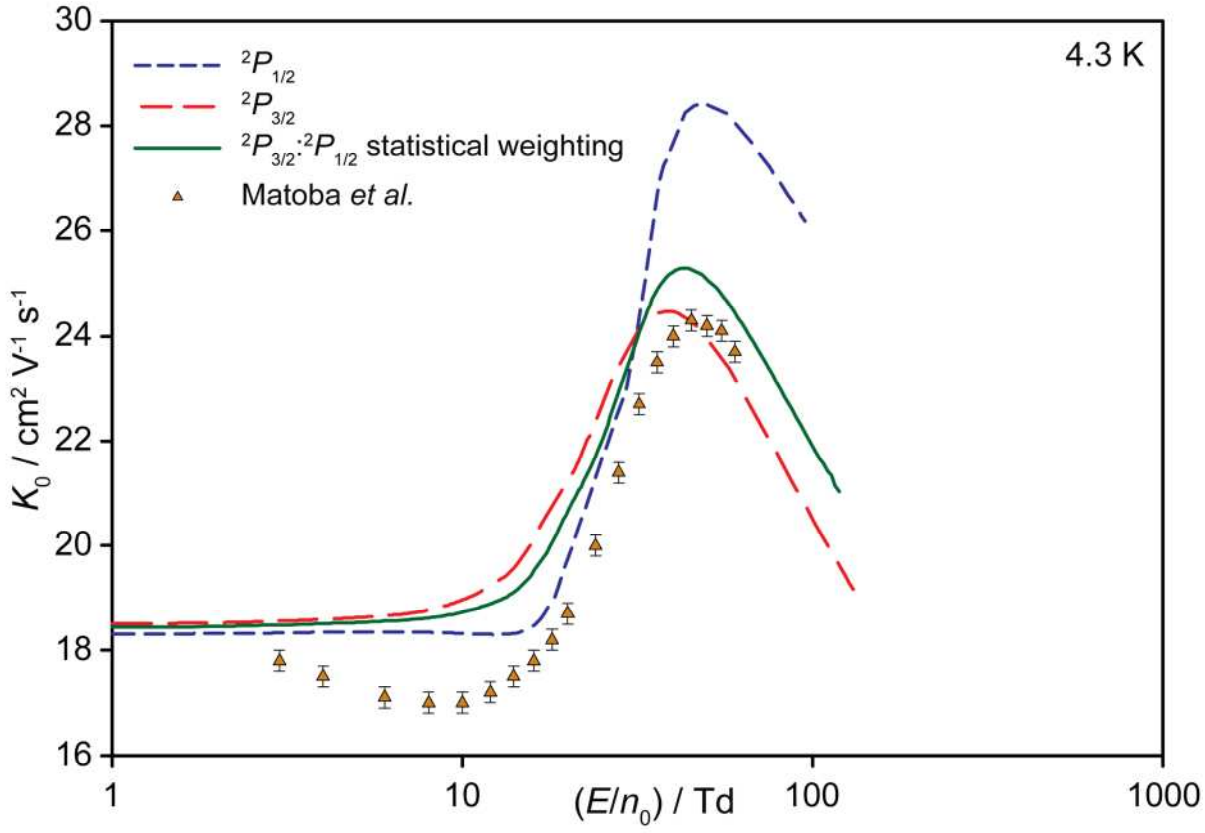

Figure 7: Comparison of the experimental and calculated $^{12}C^{+}(^{4}P_J)$ mobilities in helium at ~ 300 K, as a function of E/n_0. The points with error bars are the experimental values from Twiddy *et al.*[24]

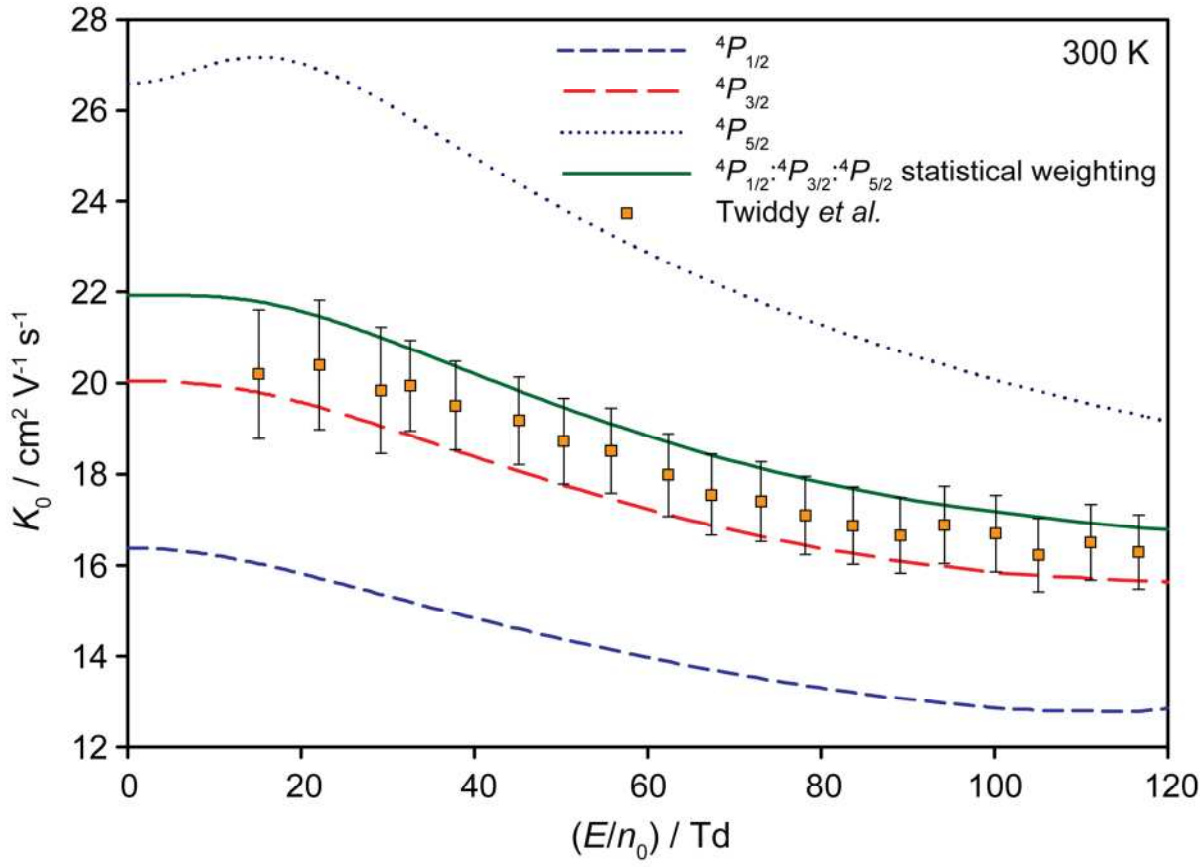

Figure 8: Comparison of the experimental and calculated $^{12}C^{+}(^{4}P_J)$ mobilities in helium at 77 K, as a function of E/n_0. The points with error bars are the experimental values from Matoba *et al.*[19]

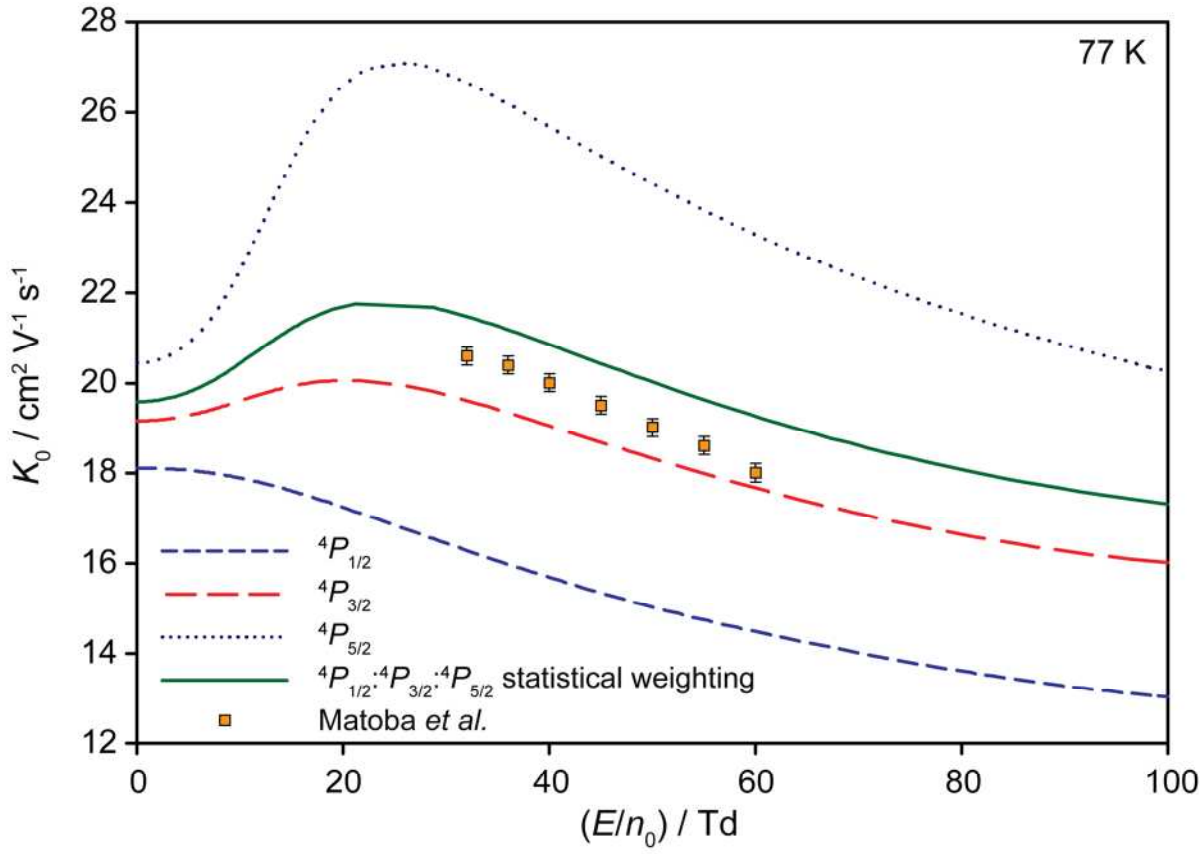

Figure 9: Comparison of the experimental and calculated $^{12}C^{+}(^{4}P_J)$ mobilities in helium at 4.3 K, as a function of E/n_0. The points with error bars are the experimental values from Matoba *et al.*[19]

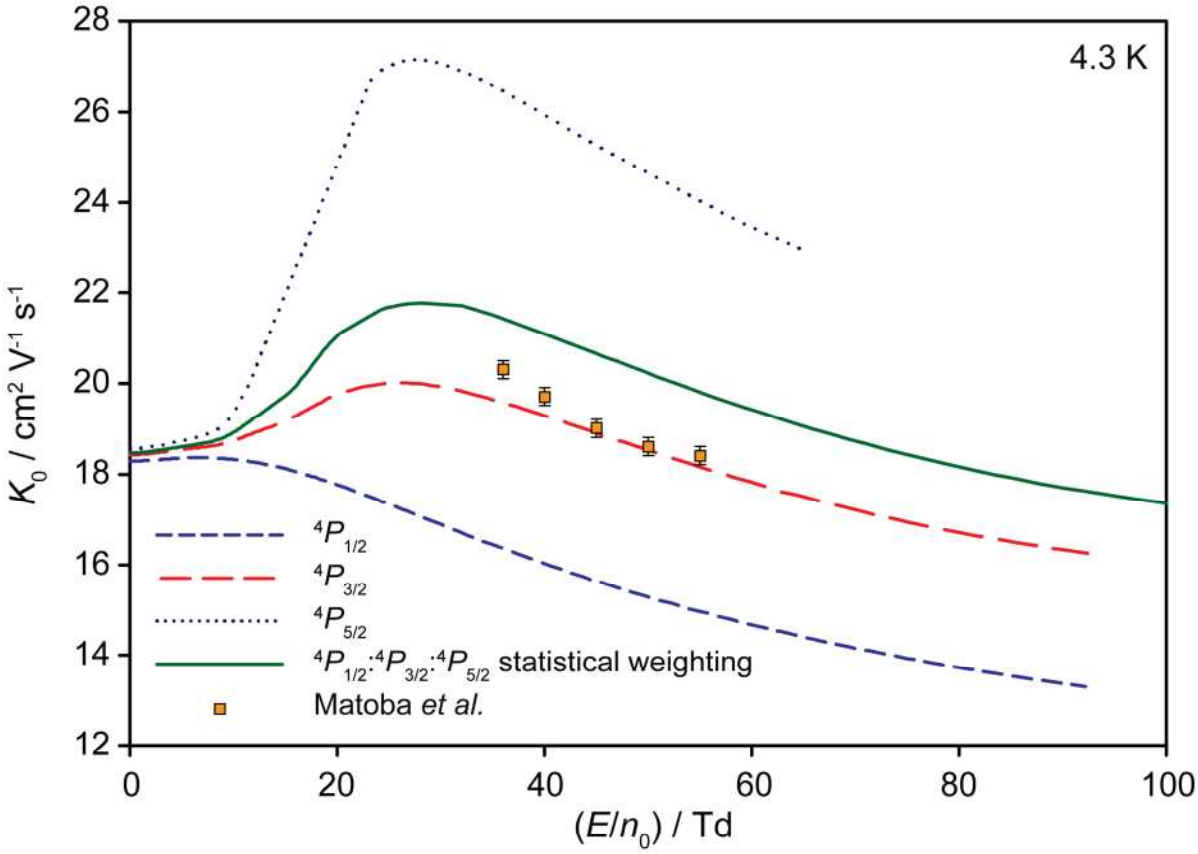

References

[1] C.G. Herbert and R.A.W. Johnstone, *Mass Spectrometry Basics* (CRC Press, Boca Raton, Fl., 2002).

[2] R.J. Lade, F. Claeyssens, K.N. Rosser and M.N.R. Ashfold, Appl. Phys. A **69**, S935 (1999).

[3] J. P.C. Grutters, A.G.H. Kessels, M. Pijls-Johannesma, D. De Ruysscher. M.A. Joore and P. Lambin, Radiotherapy and Oncology **95**, 32 (2010).

[4] S.A. Haider, M.A. Abdu, I.S. Batista, J.H. Sobral, X. Luan, E. Kallio, W.C. Maguire, M.I. Verigin, and V. Singh, J Geophys. Res. **114**, A03311 (2009).

[5] J.L. Fox and L.J. Paxton, J. Geophys. Res. **110**, A01311 (2005).

[6] S. Petrie and D.K. Bohme, Mass Spec. Rev. **26**, 258 (2007).

[7] S.W. Harrison, G.A. Henderson, L.J. Massa and P. Solomon, Astrophys. J. **189**, 605 (1974).

[8] N. Toshima, J. Phys. Soc. Jpn **38**, 1464 (1975).

[9] C. E. Moore, *CRC Series in Evaluated Data in Atomic Physics* (CRC Press, Boca Raton, Fl, 1993) p. 339.

[10] G. Herzberg, *Molecular Spectra and Molecular Structure I. Spectra of Diatomic Molecules* (Van Nostrand, New York, 1950) p. 216.

[11] D.L. Cooper and S. Wilson, Mol. Phys. **44**, 161 (1981).

[12] S.E. Young and M.J. Coggiola, Int. J. Mass Spectrom. Ion Proc. **74**, 137 (1986).

[13] W. Koch and G. Frenking, Int. J. Mass Spectrom. Ion Proc. **74**, 133 (1986).

[14] M.W. Wong, R.H. Nobes and L. Radom, J. Chem. Soc., Chem Commun. 233 (1987).

[15] G. Frenking, W. Koch, D. Cremer, J. Gauss and J.F. Liebman, J. Phys. Chem. **93**, 3397 (1989).

[16] S.T. Grice, P.W. Harland, R.G.A.R. Maclagan and R.W. Simpson, Int. J. Mass Spectrom. Ion Proc. **87**, 181 (1989).

[17] E.D. Jemmis, M.W. Wong, H.-B. Bürgi and L. Radom, J. Molec. Struct. (Theochem) **261**, 385 (1992).

[18] J.M. Hughes and E.I. von Nagy-Felsobuki, Eur. Phys. J. D **6**, 185 (1999).

[19] S. Matoba, H. Tanuma and K. Ohtsuki, J. Phys. B: At. Mol. Opt. Phys. **41**, 145205 (2008).

[20] R. Thomas, J. Barassin and A. Barassin, Int. J. Mass Spectrom. Ion Phys. **31**, 227 (1979).

[21] I. Dotan, F.C. Fehsenfeld and D.L. Albritton, J. Chem. Phys. **71**, 4762 (1979).

[22] H.W. Ellis, M.G. Thackston, E.W. McDaniel and E.A. Mason, At. Data Nucl. Data **31**, 113 (1984).

[23] N. Peska, Dissertation, Leopold-Franzens-Universität, 1981.

[24] N.D. Twiddy, A. Mohebati and M. Tichy, Int. J. Mass Spectrom. Ion Proc. **74**, 251 (1986).

[25] M. Rincon, N.J. Kirchner and M.T. Bowers, Int. J, Mass Spectrom. Ion Proc. **86**, 369 (1988).

[26] MOLPRO is a package of *ab initio* programs written by H.-J. Werner, P.J. Knowles, G. Knizia, F.R. Manby, M. Schütz, P. Celani, T. Korona, R. Lindh, A. Mitrushenkov, G. Rauhut, K.R. Shamasundar, T.B. Adler, R.D. Amos, A. Bernhardsson, A. Berning, D.L. Cooper, M.J.O. Deegan, A.J. Dobbyn, F. Eckert, E. Goll, C. Hampel, A. Hesselmann, G. Hetzer, T. Hrenar, G. Jansen, C.

Köppl, Y. Liu, A.W. Lloyd, R.A. Mata, A.J. May, S.J. McNicholas, W. Meyer, M.E. Mura, A. Nicklaß, D.P. O'Neill, P. Palmieri, D. Peng, K. Pflüger, R. Pitzer, M. Reiher, T. Shiozaki, H. Stoll, A.J. Stone, R. Tarroni, T. Thorsteinsson, M. Wang.

[27] H.-J. Werner, P. J. Knowles, G. Knizia, F.R. Manby and M. Schütz, WIREs Comput Mol Sci **2**, 242-253 (2012).

[28] K.A. Peterson and T.H. Dunning, Jr., J. Chem. Phys. **117**, 10548 (2002).

[29] D.E. Woon and T.H. Dunning, Jr. J. Chem. Phys. **100**, 2975 (1994).

[30] A. Halkier, T. Helgaker, P. Jorgensen, W. Klopper, H. Koch, J. Olsen and A.K. Wilson, Chem. Phys. Lett. **286**, 243 (1998).

[31] A. Halkier, T. Helgaker, P. Jorgensen, W. Klopper and J. Olsen, Chem. Phys. Lett. **302**, 437 (1999).

[32] A. Berning, M. Schweizer, H.-J. Werner, P.J. Knowles, and P. Palmieri, Mol. Phys., **98**, 1823 (2000).

[33] R.J. Le Roy, Level 8.0: A Computer Program for Solving the Radial Schrodinger Equation for Bound and Quasibound Levels, University of Waterloo Chemical Physics Research Report CP-663 (2007).

[34] L.A. Viehland and Y. Chang, Comput. Phys. Comm. **181**, 1687 (2010).

[35] L.A. Viehland, Chem. Phys. **70**, 149 (1982).

[36] L.A. Viehland, Chem. Phys. **85**, 291 (1984).

[37] L.A. Viehland, Comput. Phys. Comm. **142**, 7 (2001).

[38] D.M. Danailov, L.A. Viehland, R. Johnsen, T.G. Wright, A.S. Dickinson, J. Chem. Phys. **128**, 134302 (2008).

[39] L.A. Viehland, Int. J. Ion Mobil. Spec. **15**, 21 (2012).

[40] www.icecat.laplace.univ-tlse.fr

[41] J.H. Sanderson, H. Tanuma, N. Kobayashi and Y. Kaneko, J. Phys. B: At. Mol. Opt. Phys. **26**, L465 (1993).

[42] N. Saito, T.M. Kojima, N. Kobayashi and Y. Kaneko, J. Chem. Phys. **100**, 5726 (1994).

[43] H. Hidaka, S. Jinno, H. Tanuma and N. Kobayashi, J. Phys. B: At. Mol. Opt. Phys. **36**, 1515 (2003).

[44] J.H. Sanderson, H. Tanuma, N. Koyashi and Y. Kaneko, J. Phys. B: At. Mol. Opt. Phys. **27**, L433 (1994).

[45] K. Ohtsuki, M. Hananoe and M. Matsuzawa, Phys. Rev. Lett. **95,** 213201 (2005).

[46] T.M. Kojima, N. Saito, N. Kobayashi and Y. Kaneko, J. Phys. Soc. Jpn. Lett. **61**, 6 (1992).

[47] L.A. Viehland and J.J. Hurly, J. Chem. Phys. **105,** 11143 (1996).

[48] H. Tanuma, H. Fujimatsu and N. Kobayashi, J. Chem. Phys. **113**, 1738 (2000).

[49] L.A. Viehland and E.A. Mason, At. Data Nucl. Data Tables **60**, 37 (1995).

[50] L.A. Viehland, R. Webb, E.P.F. Lee and T.G. Wright, J. Chem. Phys. **122**, 114302 (2005).

[51] T.G. Wright and L.A. Viehland, Chem. Phys. Lett. **420**, 24 (2006).